OXFORD

In the face of ambiguity: intrinsic brain organization in development predicts one's bias toward positivity or negativity

Nicholas R. Harp [ID][1,*], Ashley N. Nielsen [ID][2], Douglas H. Schultz [ID][3,4], Maital Neta[3,4]

[1]Department of Psychiatry, Yale University, 300 George Street, New Haven, CT 06511, United States
[2]Department of Neurology, Washington University, 660 S. Euclid Ave., St. Louis, MO 63110, United States
[3]Department of Psychology, University of Nebraska-Lincoln, 238 Burnett Hall, Lincoln, NE 68588, United States
[4]Center for Brain, Biology, and Behavior, University of Nebraska-Lincoln, C89 East Stadium, Lincoln, NE 68588, United States
*Corresponding author: Department of Psychology, 7th Floor Suite 701, 1 Church St., New Haven, CT 06510. Email: nicholas.harp@yale.edu

Exacerbated negativity bias, including in responses to ambiguity, represents a common phenotype of internalizing disorders. Individuals differ in their propensity toward positive or negative appraisals of ambiguity. This variability constitutes one's valence bias, a stable construct linked to mental health. Evidence suggests an initial negativity in response to ambiguity that updates via regulatory processes to support a more positive bias. Previous work implicates the amygdala and prefrontal cortex, and regions of the cingulo-opercular system, in this regulatory process. Nonetheless, the neurodevelopmental origins of valence bias remain unclear. The current study tests whether intrinsic brain organization predicts valence bias among 119 children and adolescents (6 to 17 years). Using whole-brain resting-state functional connectivity, a machine-learning model predicted valence bias ($r = 0.20$, $P = 0.03$), as did a model restricted to amygdala and cingulo-opercular system features ($r = 0.19$, $P = 0.04$). Disrupting connectivity revealed additional intra-system (e.g. fronto-parietal) and inter-system (e.g. amygdala to cingulo-opercular) connectivity important for prediction. The results highlight top–down control systems and bottom–up perceptual processes that influence valence bias in development. Thus, intrinsic brain organization informs the neurodevelopmental origins of valence bias, and directs future work aimed at explicating related internalizing symptomology.

Key words: valence bias; individual differences; ambiguity; resting-state functional connectivity; machine learning.

Introduction

Internalizing disorders are prevalent and costly psychiatric disorders (Greenberg et al. 2015; Weinberger et al. 2018), and increasing rates in children and adolescents have culminated in a national emergency (American Academy of Child and Adolescent Psychiatry 2021). A shared cognitive–behavioral phenotype of internalizing disorders is an exacerbated negativity bias (Beck 1976; Williams et al. 2007; Daniel-Watanabe et al. 2022). For instance, individuals with major depressive disorder are more likely to remember negative stimuli and show a stronger negativity bias than individuals without a psychiatric diagnosis (Hamilton and Gotlib 2008; Gollan et al. 2016), and the degree of negativity scales with symptom severity (Daniel-Watanabe et al. 2022). Likewise, individuals with anxiety are more likely to remember negative information (Mitte 2008) and interpret uncertain threats as threatening (Eysenck et al. 1991; Williams et al. 2007). Thus, the characteristic negativity of internalizing disorders is a transdiagnostic feature, perhaps representing an early target for intervention or an affective risk factor informing mental health trajectories through adolescence and into emerging adulthood (Beck 1976; Silvers and Peris 2023).

Certainly, biased affective evaluations wreak havoc on rational and adaptive decision-making behavior, particularly in contexts marred by uncertainty (e.g. risk, ambiguity; Tversky and Kahneman 1971), and also adversely impact psychological well-being (Norris et al. 2011; Gollan et al. 2016). For instance, overly negative evaluations bias motivational behavior (e.g. approach–avoidance decisions; Krieglmeyer et al. 2010), limiting opportunities for positive outcomes (e.g. strengthening social bonds, novel experiences). Notably, circumstances in daily life, including social signals like facial expressions or language, are often emotionally ambiguous. That is, the same signal can convey either positive or negative valence. For example, a surprised facial expression can convey positive (e.g. unexpected party) and negative outcomes (e.g. a car accident). As a result, individuals show a stable tendency toward more positive or negative appraisals of such signals (i.e. *valence bias*; Neta et al. 2009; Neta et al. 2013; Harp et al. 2021).

Mounting evidence links a more negative valence bias to poorer well-being, including subclinical internalizing symptoms. In adulthood, a more negative valence bias is associated with more severe symptoms of depression and anxiety (Park et al. 2016; Neta and Brock 2021). Likewise, individuals with a more negative valence bias show heightened stress and emotional reactivity in both self-report and physiological measures (e.g. neuroticism, cortisol response; Brown et al. 2017; Raio et al. 2021; Brock et al. 2022). Further, feelings of loneliness (Harp and Neta 2023), lower levels of physical activity (Neta et al. 2019), and higher levels of daily negative affect (Puccetti et al. 2023)—all of which are associated with depression (Cacioppo et al. 2006; Ströhle 2009; Dunkley et al. 2017)—are linked to a more negative valence bias.

Nonetheless, the neural mechanisms driving an individual to have a more positive or negative valence bias remain unclear.

Individual differences in valence bias are thought to arise from a two-stage process characterized by an initial negative appraisal (Neta and Whalen 2010; Petro et al. 2021), which is subsequently updated with a more positive appraisal in some individuals (Neta and Whalen 2010; Neta et al. 2021). Evidence for this "initial negativity hypothesis" (Petro et al. 2018) comes, in part, from computer mouse-tracking (Freeman and Ambady 2010), in which positive responses to ambiguous stimuli are initially attracted to the competing (negative) response option (Brown et al. 2017; Neta et al. 2021). The ability to update initially negative appraisals with more positive, secondary appraisals in this way seems to be linked with the use of cognitive reappraisal as a strategy for emotion regulation (Neta et al. 2023; Harp et al. 2023). Given that adolescence is a period of rich emotional development, perhaps including the skills to override initial negativity (e.g. reappraisal; Silvers and Peris 2023), it is a likely formative period for individual differences in valence bias.

Prior work shows that children have a more negative valence bias than adults (Tottenham et al. 2013; Marusak et al. 2017). That said, negativity in early childhood is likely normative, whereas persistent negativity in later stages of development seemingly puts one at risk for internalizing disorders. For example, the link between a more negative valence bias and depression symptoms is evident after the onset of puberty (Petro et al. 2021), and neurobiological changes during puberty seemingly underlie the effect. The failure to develop a "mature" pattern of amygdala connectivity—that is suggestive of emotion regulation (Andersen and Teicher 2008; Gee et al. 2013)—confers a more negative valence bias (Petro et al. 2021) and a heightened risk for internalizing disorders (Phillips et al. 2008; Gee et al. 2013).

In adults, a task control (i.e. cingulo-opercular; Dosenbach et al. 2007) system—including the anterior insula/frontal operculum and the dorsal anterior cingulate cortex/medial superior frontal cortex—plays a critical role in response to ambiguity (Thompson-Schill et al. 1997; Sterzer et al. 2002; Neta et al. 2013, 2016). The cingulo-opercular system is crucial for the stable maintenance of the task set (Dosenbach et al. 2007) and for monitoring ongoing task performance, particularly in challenging situations (e.g. conflict, ambiguity; see Gratton et al. 2017; Neta et al. 2014, 2016). With relevance for valence bias, cingulo-opercular regions show greater activity when judging the valence of emotionally ambiguous stimuli (i.e. resolving the ambiguity) compared to nonvalence judgments (i.e. ambiguity may not even be detected; Neta et al. 2013). Thus, the cingulo-opercular system represents another putative source of control or regulation that could shape individual differences in valence bias.

Because each of these systems—(i) cortical regions functionally connected with the amygdala and (ii) the cingulo-opercular system—could shape an individual's valence bias, we consider the intrinsic organization within each system, between the two systems, and with other functional systems (e.g. the visual system). Intrinsic organization is often characterized via resting-state functional connectivity (RSFC; Bullmore and Sporns 2009; Power et al. 2011), which captures the history of coactivation among brain regions throughout an individual's life (Fox and Raichle 2007), perhaps related to ongoing learning and memory processing (i.e. offline plasticity; Laumann and Snyder 2021). That is, variation in RSFC has the potential to inform individual differences in behavior, and, in concert with machine learning algorithms, is showing increasing promise for identifying "connectome fingerprints" (Finn et al. 2015). RSFC can be leveraged to predict

characteristics like age (Nielsen et al. 2019), sex (Casanova et al. 2012), IQ (Santarnecchi et al. 2014), and clinical outcomes (e.g. depression status; Craddock et al. 2009). Because the organization of both cortico-amygdala connectivity (Andersen and Teicher 2008; Gee et al. 2013) and the cingulo-opercular system (Nielsen et al. 2019) undergo substantial changes throughout development, there may be unique patterns of resting-state connectivity that underpin age-related differences in valence bias (Petro et al. 2021).

Here, we evaluated the contributions of RSFC, particularly in (i) cortical regions coupled with the amygdala and (ii) the cingulo-opercular system, to the prediction of valence bias in a sample of children and adolescents. We used a machine learning algorithm to predict valence bias, using approaches that identified the predictive utility of RSFC at several scales (e.g. intra-system, inter-system, system-free regions). Although we had specific hypotheses, we began with a whole-brain approach. Then, we used a hypothesis-driven examination of RSFC among regions coupled with the amygdala as well as the cingulo-opercular system, both jointly and individually. Finally, we probed the role of functional brain systems in a more exploratory, hypothesis-free fashion by selectively disrupting the relationship between functional connectivity (at the system-, block-, and region of interest [ROI] level) and valence bias in permutation sensitivity analyses (PSAs). Our results inform the neurodevelopmental origins of individual differences in valence bias that may illuminate variability in subclinical internalizing symptomology.

Materials and methods
Participants

We recruited 192 children from the Lincoln, Nebraska community. Of these, 160 completed a prescanning session, including an assessment of valence bias (described below) and a scanning session approximately 1 week later. Of these 160 participants, 41 were excluded prior to analysis due to completing a different version of the valence bias task ($n = 11$; i.e. only including faces), having an inadequate amount of data retained after motion censoring ($n = 13$; described below), failure of alignment and registration of the imaging data into the target atlas space ($n = 13$), or inaccurate responses in the valence bias task ($n = 4$; see below). The final sample included 119 participants [$M(SD)_{age} = 10.60(2.93)$, range = 6 to 17; 63 female, 56 male; 2 Asian, 6 Black, 98 White, 12 more than one race, 1 unknown race; 12 Hispanic/Latino, 106 not Hispanic/Latino, 1 unknown ethnicity]. All participants (and their legal guardian) confirmed understanding of the procedures and provided written informed consent. All procedures were approved by the local institutional review board.

Procedure

In a prescanning session, participants completed the valence bias task, followed by a series of questionnaires beyond the scope of the present report (see Supplemental Materials, Table S1) and then by a mock scan. The valence bias task was completed in either E-Prime (Psychology Software Tools, Pittsburgh, PA, USA) or MouseTracker (Freeman and Ambady 2010). As in previous work (Neta et al. 2009, 2013), participants completed a two-alternative forced choice task in which images were categorized as either positive or negative. The task comprised four blocks (two faces, two scenes), each with 12 ambiguous and 12 clear trials (6 positive, 6 negative), for a total of 96 trials (48 ambiguous, 48 clear). The faces included 34 discrete identities taken from the NimStim (14 identities, 7 females, age 21 to 30 years; Tottenham et al. 2009) and Karolinska Directed Emotional Faces (20 identities, 10

females, age 20 to 30 years; Lundqvist et al. 1998) sets, displaying happy, angry, or surprised expressions. The scenes were selected from the International Affective Picture System (Bradley and Lang 2007) and were previously validated as being emotionally ambiguous (Neta et al. 2013; Harp et al. 2021). The clearly positive and negative images were used as within-subjects controls, such that accuracy falling below 60% resulted in exclusion from the study ($n = 1$ for inaccurate responses to positive images, $n = 3$ for inaccurate responses to negative images), as in prior work (Harp et al. 2021; Neta et al. 2019, 2023). Valence bias was calculated as the percentage of negative categorizations for ambiguous faces and scenes, excluding omissions (Neta et al. 2009).

Approximately 1 week after the pre-scanning session, participants were invited to return for the scanning session. Functional scans included a passive face viewing task, an emotion regulation task, and a resting-state scan (see Petro et al. 2021 for task details), during which participants passively viewed a white crosshair on a black background.

Image acquisition

Data were collected on a Siemens 3T Skyra scanner housed within the Center for Brain, Biology, and Behavior at University of Nebraska—Lincoln. Structural images were collected using a T1-weighted MP-RAGE sequence (TR = 2.2 s, TE = 3.37 ms, slices = 192 interleaved, 1 mm isotropic voxel size, FOV = 256 mm, flip angle = 7 degrees, total acquisition time = 5:07). Two sets of imaging parameters were used for resting-state functional scans [*Cohort 1* ($n = 30$): TR = 2.5 s, TE = 30 ms, slices = 42 interleaved, voxel size = 2.5 × 2.5 × 2.8 mm, matrix = 88 × 88 mm, FOV = 220 mm, flip angle = 80°; *Cohort 2* ($n = 89$): TR = 1.0 s, TE = 30 ms, slices = 51, voxel size = 2.5 mm isotropic, matrix = 84 × 84 mm, FOV = 210 mm, flip angle = 41°, multiband factor = 8]. Resting-state scans were collected over three runs, each approximately 5 min in length for a total of approximately 15 min of resting-state scanning.

Image preprocessing

Structural and functional images were registered to a target atlas in Talairach space (Talairach and Tournoux 1988) created from MP-RAGE scans of thirteen 7- to 9-year-old children (7 males) and twelve 21- to 30-year-old adults (6 males) scanned on a Siemens 3T MAGNETOM Trio scanner (TRIO_KY_NDC). Coregistration of functional to anatomical images was completed with Freesurfer. In the event of alignment failures, Analysis of Functional Neruoimaging's (AFNI) align_epi_anat script was used with big, giant, or ginormous moves. Subjects for which this failed to resolve the alignment issue were removed ($n = 13$). After conforming the structural scans to the target atlas space, cortical reconstruction was completed in Freesurfer with the recon-all command (Dale et al. 1999); then, scans were registered to fs_LR surface space (Van Essen et al. 2012) and aligned with functional data for functional connectivity processing (Gordon et al. 2016).

Functional connectivity processing

Functional connectivity processing included demeaning and detrending of each functional run, regression of nuisance variables (i.e. global signal, cerebrospinal and white matter nuisance masks derived from Freesurfer and six rigid-body motion parameters, motion derivatives, and Volterra expansion of motion estimate; Friston et al. 1996), frame censoring and interpolation of data within runs (discussed below), a temporal band-pass filter ($0.009\ Hz < f < 0.08\ Hz$), and spatial smoothing (6 mm full width at half maximum). To reduce motion-related artifacts, framewise motion censoring, and global signal regression, a well-validated procedure for reducing head motion–related artifacts (Power et al. 2014), were implemented. More specifically, preprocessing realignment estimates were used to determine framewise displacement (FD), and frames with greater than 0.2 mm FD were censored (removed) prior to analysis (see Power et al. 2014; Nielsen et al. 2019). After framewise censoring, data segments with less than five contiguous frames were removed. The remaining number of frames from any given functional run needed to reach at least 50 frames to be included in the analysis.

ROIs

We extracted RSFC time series from 264 whole-brain ROIs (10 mm diameter; Power et al. 2011). Then, we correlated the time series from each ROI to produce a correlation matrix, normalized using a Fisher z-transform, representing each individual's RSFC. RSFC from these ROIs revealed organization of separable functional systems, consistent with extensive previous research (e.g. Dworetsky et al. 2021; Nielsen et al. 2019; Power et al. 2011; Yeo et al. 2011). In addition to these ROIs, a task-based amygdala "system" that included 26 additional ROIs (10 mm diameter) was defined using a seed-based approach and added to the set of 264 ROIs (Power et al. 2011). We defined this amygdala system to provide coverage of bilateral amygdala and functionally connected regions (i.e. "amygdala network"), given prior work linking amygdala–prefrontal coactivity to individual differences in valence bias (Petro et al. 2021).

The two seeds, one in left (Talairach: −20, −2, −13) and one in right (Talairach: 32, 2, −16) amygdala, were identified based on task activation in prior work (Petro et al. 2018). Resting-state functional runs were concatenated using 3dTcat in AFNI, and every remaining voxel in the brain (i.e. any voxel outside the seed regions) was correlated with both seed regions. Group-level statistics were completed using AFNI's 3dttest++ and the clustsim option to correct for multiple comparison (Cox et al. 2017). Cluster thresholds were then applied using AFNI's 3dClusterize (Cox et al. 2017), and spherical ROIs were created at the center of mass coordinates of surviving clusters. The ROIs then significantly correlated—positively or negatively—with the amygdala seed regions were plotted to the brain and examined for overlap with the 264 ROIs described above. This resulted in 26 clusters correlated with the left amygdala and 23 clusters correlated with the right amygdala (49 clusters + 2 seeds = 51 total). Eleven of the ROIs from either the left or right amygdala group were overlapping with another amygdala-derived ROI (e.g. a cluster correlated with the left amygdala overlapped with a cluster correlated with the right amygdala); thus, we removed one of the overlapping ROIs from each pair (left vs. right at random). Fourteen of the remaining ROIs overlapped with one of the already existing 264 ROIs (Power et al. 2011). After removing the 14 overlapping ROIs (see Table S2), the remaining 26 ROIs (10 mm diameter) were combined with the set of Power et al.'s (2011) 264 ROIs. Altogether, there were 290 ROIs.

Support vector regression

Support vector regression (SVR), an extension of support vector machines, leverages multivariate (e.g. RSFC) patterns to optimize a model for predicting continuous labels. Specifically, the patterns among a set of features (here, 41,905 functional connections among 290 ROIs—or some subset of these features) and labels (here, observed valence bias) in a training sample are used to build a model that is applied to a testing sample. To do this, 10-fold cross-validation (CV) was used, such that in each fold, the

SVR model was built using 90% of the sample and then patterns identified in the training sample were tested on the remaining 10% of the sample, and this process is repeated 10 times. To assess performance of the SVR models, we report the correlation between observed and predicted valence bias in the full sample using Spearman's rho. We implemented two feature interrogation approaches: (i) feature selection and (ii) feature permutation.

Feature interrogation

Because SVR models combine complex information across multiple features, it is challenging to directly interpret the relative importance of single features without further interrogation. As such, we implemented both targeted, hypothesis-driven (feature selection) and brain-wide, hypothesis-free (feature permutation) feature interrogation approaches that manipulate the features available for SVR and measure the impact on prediction. More specifically, a targeted, hypothesis-driven approach to feature interrogation is feature selection, that is, selecting and testing a model using only hypothesized features associated with ROIs assigned to functional systems of a priori interest (e.g. connections shared with cingulo-opercular system ROIs). As such, one can determine whether the connections associated with a system of interest is sufficient for constructing a predictive model. Conversely, a brain-wide, hypothesis-free approach to feature interrogation might iteratively examine the importance of each functional system by selectively permuting the data used for testing to disrupt features associated with a given functional system and measuring the impact on prediction. This approach is known as feature permutation and can determine whether the connections associated with a system are necessary for constructing a predictive model.

Feature selection

First, we determined whether using only connections that had at least one ROI in the two a priori systems of interest (amygdala, cingulo-opercular)—either jointly or independently— as features was sufficient for prediction of valence bias. To determine whether the model built on the reduced feature set performed well, we correlated observed and predicted valence bias values.

Permutation sensitivity

Second, we implemented a more hypothesis-free brain-wide feature interrogation by testing the impact of selectively disrupting connections on the prediction of valence bias. If a set of features is important for predicting valence bias, permuting the true values of these features would negatively impact prediction. We tested whether the brain-wide patterns of functional connectivity that predict valence bias were sensitive to disruptions at the level of: (i) systems (i.e. inter- *and* intra-system connectivity for each functional system), (ii) blocks (i.e. inter-system connectivity for any single system *or* intra-system connectivity for any two systems), and (iii) ROIs (i.e. a system agnostic approach that assessed connectivity involving a single ROI; Nielsen et al. 2022). See Fig. 3C for a visual depiction of each level of permutation and the Supplementary Materials for pseudocode.

In the first step, the relationship between the participants' observed valence bias and the targeted features were permuted for the test set in each fold of the cross-validation. Estimates of valence bias were then generated using the SVR model for the subjects in the test set with permuted features. This provides a permuted R^2 value (averaged across CV folds) which is subtracted from the R^2 value of the full, unpermuted model. This provides

Table 1. Covariate models.

Covariate	Spearman's rho	P
Age	0.20	0.03
Motion (percent frames retained)	0.25	0.005
Experimental software	0.26	0.005
Sequence acquisition parameters	0.20	0.03
Full model (age, motion, sequence)	0.22	0.02

Note: Results of the SVR model when accounting for various covariates. The full model could not include both the scanning parameters (sequence) and experimental software given high levels of colinearity [$r(117) = 0.90$, $P < 0.001$].

ΔR^2. Negative ΔR^2 values represent worsened prediction after disrupting the relationship between individuals' valence bias and their pattern of functional connectivity.

In the second step, in order to interpret differences in performance between systems/blocks that are related to the different number of features across different systems and blocks (Nielsen et al. 2020), 1,000 size-matched, randomly selected feature sets were generated as comparisons for each system-level and block-level analysis. For example, the performance of the amygdala system (26 ROIs and their connections) would be compared to the performance of 1,000 size-matched sets of randomly selected features (26 ROIs and their connections). This same strategy was applied to the block-level analyses. Given that the ROI-level includes only a single ROI and all its connections, a single set of one thousand permutations were used for the null comparison. The results of the ROI-level analysis are in the Supplemental Material (Table S3, Table S4).

Results
Individual differences in valence bias are associated with patterns of whole-brain RSFC

First, we tested whether 10-fold CV SVR could predict individual differences in valence bias [$M(SD) = 53.87$ (18.49), range = 8.33 to 87.14; Fig. 1A] using patterns of whole-brain RSFC. That is, this model used all 41,905 functional connections (edges) from the 290 ROIs (nodes; Fig. 1B and C). This whole-brain SVR captured a significant proportion of the variance in valence bias [$r_s(117) = 0.20$, $P = 0.03$; $R^2 = 0.03$].

We also tested for potential confounds, including age, percentage of high motion frames, software, sequence acquisition parameters, and a model accounting for several of these covariates (experimental software and sequence acquisition parameters were too colinear for inclusion in a single model); none of these accounted for the model's ability to predict valence bias (see Table 1). We also attempted prediction of age ($r_s = 0.78$, $P < 0.001$) and percentage of correct negative categorizations for the clearly positive ($r_s = 0.16$, $P = 0.07$) and clearly negative ($r_s = 0.25$, $P = 0.007$) images. Although the model successfully predicted categorizations of negative images, accounting for age in the same model resulted in nonsignificant, inverted predictions ($r_s = -0.09$, $P = 0.31$). Altogether, the pattern of results indicate that these potential confounding variables do not explain the model's ability to predict valence bias.

Using RSFC in the amygdala and cingulo-opercular systems to predict valence bias

Next, we built models using a subset of connections with at least one node in either of the two a priori systems of interest: (i) combined amygdala and cingulo-opercular systems,
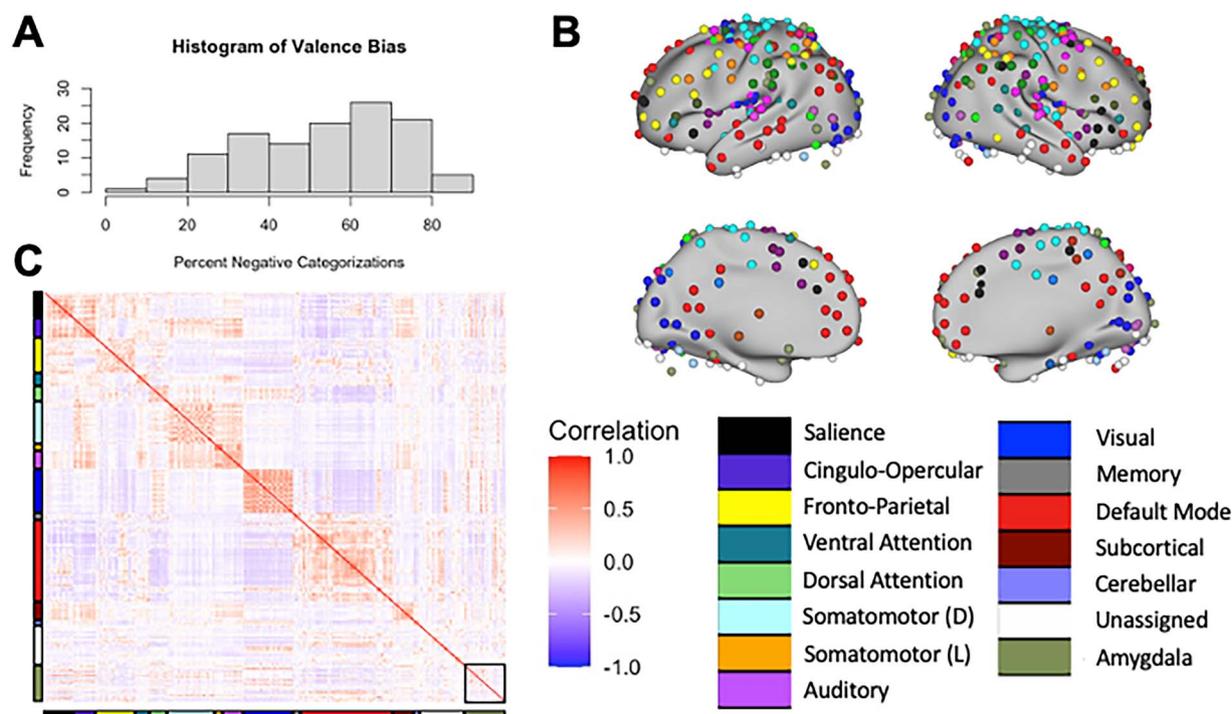
Fig. 1. Whole-brain resting-state functional connectivity. A) Histogram of valence bias. B) 290 ROIs (nodes) distributed across the cortex. C) Average correlation matrix ($n = 119$ children) depicting strength of connections (edges) among all 290 ROIs (nodes). The amygdala system is outlined in the bottom right of the matrix.
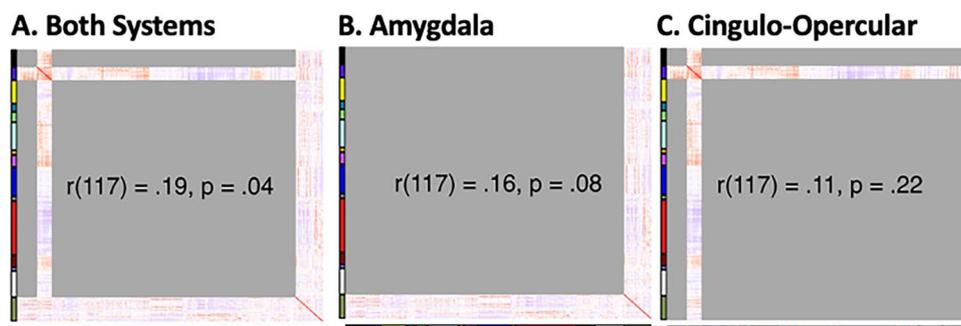

Fig. 2. Hypothesis-driven feature selection. Visualization of feature selection and feature masking (gray) for analyses of the a priori systems of interest. Because the RSFC matrix is symmetric, there are redundant features across the diagonal, in the upper and lower halves of the matrix.

(ii) amygdala system alone, and (iii) cingulo-opercular system alone. The combined model predicted valence bias [$r_s(117) = 0.19$, $P = 0.04$, $R^2 = 0.04$; Fig. 2A]. However, neither the amygdala [$r_s(117) = 0.16$, $P = 0.08$, $R^2 = 0.03$; Fig. 2B] nor cingulo-opercular system [$r_s(117) = 0.11$, $P = 0.22$, $R^2 = 0.02$; Fig. 2C] alone were sufficient for predicting bias.

Multiple functional systems are important for predicting valence bias

Next, we explored the impacts of perturbing connections of a given functional system in a brain-wide, hypothesis-free manner. Multiple functional systems predicted valence bias (see Table 2, Fig. 3A). The cingulo-opercular ($\Delta R^2 = -0.010$, $P < 0.001$), fronto-parietal ($\Delta R^2 = -0.013$, $P < 0.001$), visual ($\Delta R^2 = -0.013$, $P = 0.02$), and subcortical systems ($\Delta R^2 = -0.009$, $P < 0.001$) emerged as significant contributors, in that permuting their connections significantly impaired predictive power. Disrupting the remaining functional systems, however, including the amygdala system, did not significantly impair prediction.

Neurobiological correlates of valence bias are distributed across functional systems

To further specify the contribution of intra-system connectivity (i.e. among ROIs within the same functional system) and inter-system connectivity (i.e. among ROIs from two separate functional systems), the connections among ROIs within a single system or between two separate systems were tested against random permutations of these connections. Interestingly, with the exception of the fronto-parietal system ($\Delta R^2 = -0.002$, $P < 0.001$) and unassigned system ($\Delta R^2 = -0.002$, $P < 0.001$), the functional systems contributing to prediction at the system level appear to be primarily driven by between-system connectivity (see Fig. 3B). For example, connectivity between the cingulo-opercular and the fronto-parietal ($\Delta R^2 = -.001$, $P < 0.001$), visual ($\Delta R^2 = -0.005$, $P < 0.001$), and amygdala systems ($\Delta R^2 = -.002$, $P < 0.001$) significantly contributed to prediction. The visual system also showed effects of inter-system connectivity with the dorsal attention ($\Delta R^2 = -0.002$, $P < 0.001$) and frontoparietal systems ($\Delta R^2 = -0.002$, $P < 0.001$). See Table 3 for additional block-level ΔR^2 values.

Fig. 3. System- and block-level PSAs. A) The diamonds represent the change in prediction when features of a given functional system are permuted. Dots represent the distribution of 1,000 permutations for size-matched, randomly selected feature sets (i.e. the null comparison). The dashed line at 0 represents the R^2 without permutation. Stars indicate systems for which permutation significantly impaired prediction (i.e. negative change in ΔR^2, $P < 0.05$). B) Results of the block-level PSAs. Solid, filled blocks were significantly impacted following permutation ($P < 0.05$), whereas shaded blocks ($.05 < P < 0.10$) and unfilled blocks ($P > 0.10$) did not. C) From left to right, depictions of the features selected for system-level, block-level, and ROI-level PSAs. At the system level, all features associated with a single functional system are selected for permutation. At the block level, sets of features within a single functional system (e.g. somatomotor dorsal to somatomotor dorsal) or between two functional systems (e.g. somatomotor dorsal to visual) are selected for permutation. Lastly, at the system agnostic ROI level, the connections of a single ROI are selected for permutation. Note that, because the matrix is symmetrical, SVR would only use the first instance of each feature (i.e. edge/connection), removing redundancy across the matrix diagonal. SAL, salience; CO, cingulo-opercular; FP, fronto-parietal; VEN ATT, ventral attention; DOR ATT, dorsal attention; SM (D), somatomotor (dorsal); SM (L), somatomotor (lateral); AUD, auditory; VIS, visual; MEM, memory; DM, default mode network; SUBCor, subcortical; CEREB, cerebellum; UNASGN, unassigned; AMYG, amygdala.

Table 2. Results of PSAs at the system level.

Functional system	ΔR^2	P (FDR-corrected)
Salience	0.011	> 0.99
Cingulo-opercular	**−0.010**	**< 0.001**
Fronto-parietal	**−0.013**	**< 0.001**
Ventral attention	0.002	> 0.99
Dorsal attention	−0.005	0.13
Somatomotor (D)	−0.002	> 0.99
Somatomotor (L)	0.003	> 0.99
Auditory	−0.004	0.23
Visual	**−0.013**	**0.02**
Memory	−0.003	0.11
Default mode network	−0.005	> 0.99
Subcortical	**−0.009**	**< 0.001**
Cerebellar	−0.001	0.67
Unassigned	−0.010	0.08
Amygdala	−0.009	0.11

Discussion

Exacerbated negativity is a common cognitive–behavioral phenotype of internalizing disorders (Beck 1976; Williams et al. 2007; Daniel-Watanabe et al. 2022) and can be captured by variability in response to ambiguity (i.e. valence bias; Park et al. 2016; Neta and Brock 2021). Here, we show that intrinsic brain organization can be used to predict this phenotype in a sample of healthy children and adolescents. After using a whole-brain approach, we tested a priori hypotheses that (i) regions functionally connected to the amygdala and (ii) the cingulo-opercular system would be sufficient for building a multivariate predictive model of valence bias. Although the amygdala- and cingulo-opercular-based models were insufficient, the joint amygdala and cingulo-opercular model successfully predicted valence bias. In a series of permutation analyses, we also found evidence for a role of the cingulo-opercular system, in addition to the fronto-parietal, visual, and subcortical systems (i.e. caudate nucleus, thalamus, globus pallidus, putamen, and brainstem). Further, we identified important "blocks" of inter-system connectivity, providing a more fine-grained analysis of the connectivity across the whole brain. The results further our understanding of the neural basis of exacerbated negativity common to internalizing disorders, shedding light on the neurodevelopmental origins of valence bias and providing clinical insight into the neural basis of a common phenotype of internalizing disorders.

Neurodevelopmental origins and the mechanistic account of valence bias

As hypothesized, RSFC among regions functionally connected to the amygdala and the cingulo-opercular system (Dosenbach et al. 2007; Power et al. 2011) predicted individual differences in valence bias. However, restricting the feature set to include only connections with a node in either of the two systems was insufficient for prediction. That said, the cingulo-opercular system emerged as a significant contributor to prediction in the system-level PSAs, and cingulo-opercular to amygdala functional connectivity emerged as important for prediction in the block-level PSA. Previous findings implicate the cingulo-opercular system as a key system for valence bias in adults (Neta et al. 2013), and the resolution of ambiguity more broadly (Thompson-Schill et al. 1997; Sterzer et al. 2002; Neta et al. 2014, 2016; Gratton et al.

2017), but the present findings provide the first evidence that the same task-control system is linked to valence bias in children. Because patterns of cingulo-opercular connectivity are useful for predicting age, even within the first month of life (Nielsen et al. 2022), the predictive utility of the cingulo-opercular system may, at least in part, be attributable to developmental changes in cingulo-opercular connectivity (Nielsen et al. 2019). That said, the model remained predictive of valence bias when controlling for age, among other possible confounding variables. Though the present findings are cross-sectional, future research could characterize how cingulo-opercular connectivity and valence bias change together throughout development.

Permutation analyses also indicated other functional systems important for predicting valence bias, especially the visual system, which emerged as a significant contributor in both system- and block-level PSAs. This corroborates behavioral evidence that manipulations of visual input modulate valence bias (Neta et al. 2017; Neta and Dodd 2018). For example, a visual spotlight paradigm, in which participants view faces "through the eyes" of someone with a highly positive or negative valence bias, revealed that the perceptual input associated with a particular bias resulted in a congruent shift in the viewers' own categorizations (e.g. more positive ratings when viewing through the eyes of someone with a more positive bias; Neta and Dodd 2018). The role of the visual system in prediction also parallels recent findings of primary sensory cortices in prediction of visual, auditory, and somatosensory domain-specific negative affect (Čeko et al. 2022). Further, emotion category-specific visual features are encoded in activity patterns distributed throughout the human visual system; that is, emotional features can be decoded both from emotional images themselves, as well as brain activity measured during participants' viewing of the images (Kragel et al. 2019). Thus, visual system organization—especially in conjunction with task-control systems—plays an important role in shaping mental representations of emotional ambiguity.

Indeed, the block-level analysis revealed that the connectivity shared among the visual system with the cingulo-opercular, fronto-parietal, and dorsal attention systems seem to be particularly important for prediction. The current mechanistic account of valence bias—the initial negativity hypothesis (Petro et al. 2018; Neta et al. 2021)—posits that regulatory processes override an initial negativity in response to emotional ambiguity. Interactions of the visual system with the cingulo-opercular, fronto-parietal, and dorsal attention systems might be the neural substrate through which the regulatory process occurs, at least in childhood/adolescence, as regions of the cingulo-opercular system communicate with downstream processors in occipital cortex (e.g. fusiform and extrastriate cortex) and the frontoparietal system exerts top–down attentional control (Dosenbach et al. 2007, 2008). Thus, the two control systems are well situated to contribute to individual differences in valence bias via influence of the task set and visual processing. Further, areal graphs of these functional systems show that the cingulo-opercular, fronto-parietal, and dorsal attention systems cluster relatively close together and are centrally located in the network of brain systems relative to more specialized processing systems (e.g. visual; Power et al. 2011). Altogether, these systems may collectively integrate the regulatory processes that give rise to individual differences in valence bias (i.e. orienting attention, generating (re)appraisals, maintaining/choosing among appraisals; Neta and Dodd 2018; Neta et al. 2023).

It is somewhat surprising that there was relatively little evidence for involvement of the amygdala system, with the

Table 3. Results of PSAs at the block level.

System	SAL	CO	FP	VEN ATT	DOR ATT	SM HAND	SM MOUTH	AUD	VIS	MEM?	DMN	SUBCor	CEREB	UNASGN	AMYG
SAL	0.001 / .99	0.000 / .99	−0.001 / .22	−0.001 / <0.001	0.001 / .99	0.000 / .99	0.000 / .99	0.001 / .99	−0.001 / .43	0.000 / .99	0.006 / .99	0.000 / .99	0.000 / .56	0.002 / .99	0.001 / .99
CO	0.000 / .99	0.000 / .99	−0.001 / <0.001	−0.001 / .48	−0.001 / .54	0.000 / .99	0.000 / .99	0.000 / .99	−0.005 / <0.001	0.000 / .99	−0.002 / .29	−0.001 / .12	0.000 / .59	0.000 / .99	−0.002 / <0.001
FP	−0.001 / .22	−0.001 / <0.001	−0.002 / <0.001	0.000 / .99	0.000 / .99	−0.001 / .59	0.000 / .71	0.000 / .99	−0.002 / <0.001	−0.001 / <0.001	0.001 / .99	−0.001 / .58	0.000 / .99	0.000 / .88	−0.001 / .63
VEN ATT	−0.001 / <0.001	−0.001 / .48	0.000 / .99	0.000 / .99	0.000 / .29	−0.001 / <0.001	0.000 / .99	0.000 / .99	0.001 / .99	0.000 / .95	0.003 / .99	−0.001 / .37	0.000 / .99	0.001 / .99	0.000 / .99
DOR ATT	0.001 / .99	−0.001 / .54	0.000 / .99	0.000 / .29	0.000 / .99	0.001 / .99	0.000 / .99	−0.001 / .56	−0.002 / <0.001	0.001 / .99	−0.001 / .58	0.000 / .99	0.000 / .99	−0.001 / .56	−0.001 / .43
SM (D)	0.000 / .99	0.000 / .99	−0.001 / .59	−0.001 / <0.001	0.001 / .99	0.000 / .99	0.001 / .99	0.001 / .99	0.000 / .99	0.001 / .99	0.000 / .99	0.001 / .99	−0.002 / <0.001	−0.001 / .99	0.000 / .99
SM (L)	0.000 / .99	0.000 / .99	0.000 / .71	0.000 / .99	0.000 / .99	0.001 / .99	0.000 / .99	0.000 / .99	0.001 / .99	0.000 / .99	0.000 / .99	0.000 / .99	0.000 / .80	0.000 / .99	0.000 / .99
AUD	0.001 / .99	0.000 / .99	0.000 / .99	0.000 / .99	−0.001 / .56	0.001 / .99	0.000 / .99	0.000 / .99	0.001 / .99	0.000 / .99	−0.003 / <0.001	−0.002 / <0.001	0.000 / .99	0.000 / .99	0.000 / .85
VIS	−0.001 / .43	−0.005 / <0.001	−0.002 / <0.001	0.001 / .99	−0.002 / <0.001	0.000 / .99	0.001 / .99	0.001 / .99	0.003 / .99	0.000 / .71	−0.001 / .99	−0.001 / .92	0.001 / .99	−0.002 / .58	−0.002 / .12
MEM	0.000 / .99	0.000 / .99	−0.001 / <0.001	0.000 / .95	0.001 / .99	0.001 / .99	0.000 / .99	0.000 / .28	0.000 / .71	0.000 / .82	−0.001 / .22	0.000 / .99	0.000 / .89	0.000 / .89	−0.001 / .12
DMN	0.006 / .99	−0.002 / .29	0.001 / .99	0.003 / .99	−0.001 / .58	0.000 / .99	0.000 / .99	−0.003 / <0.001	−0.001 / .99	−0.001 / .22	0.003 / .99	−0.002 / .12	0.000 / .99	−0.005 / <0.001	−0.001 / .99
SUBCor	0.000 / .99	−0.001 / .12	−0.001 / .58	−0.001 / .37	0.000 / .99	0.001 / .99	0.000 / .99	−0.002 / <0.001	−0.001 / .92	0.000 / .99	−0.002 / .12	0.000 / .48	−0.001 / .12	−0.001 / <0.001	−0.001 / .82
CEREB	0.000 / .56	0.000 / .59	0.000 / .99	0.000 / .99	0.000 / .99	0.000 / .99	0.000 / .80	0.000 / .99	0.001 / .99	0.000 / .89	0.000 / .99	−0.001 / .12	0.000 / .99	0.000 / .99	0.000 / .59
UNASGN	0.002 / .99	0.000 / .99	0.000 / .88	0.001 / .99	−0.001 / .56	−0.001 / .99	0.000 / .99	0.000 / .99	−0.002 / .58	0.000 / .89	−0.005 / <0.001	−0.001 / .99	0.000 / .99	−0.002 / .99	0.000 / .99
AMYG	0.001 / .99	−0.002 / <0.001	−0.001 / .63	0.000 / .99	−0.001 / .43	0.000 / .99	0.000 / .99	0.000 / .85	−0.002 / .12	−0.001 / .12	−0.001 / .99	−0.001 / .82	0.000 / .59	−0.001 / <0.001	0.000 / .99

Note: Delta R^2 (upper) and *P*-values (lower; FDR-corrected) are shown in each cell. Bold cells indicate significant FDR-corrected *p*-values ($p < .05$). SAL, salience; CO, cingulo-opercular; FP, fronto-parietal; VEN ATT, ventral attention; DOR ATT, dorsal attention; SM (D), somatomotor (dorsal); SM (L), somatomotor (lateral); AUD, auditory; VIS, visual; MEM, memory; DMN, default mode network; SUBCor, subcortical; CEREB, cerebellum; UNASGN, unassigned; AMYG, amygdala.

exception of the amygdala to cingulo-opercular block. For example, one might expect the amygdala–visual system block to emerge as a significant contributor to the models, given evidence of feedback projections from the amygdala to occipital cortex that modulate visual perception (Amaral et al. 2003). One possibility is that, because the primary parcellation scheme used here did not include amygdala (Power et al. 2011), our task-based amygdala system could only include regions not already assigned to another functional system. In other words, regions relevant to regulating amygdala activity in the context of valence bias, like the ventromedial prefrontal (Kim et al. 2003; Petro et al. 2021) or lateral prefrontal cortex (Petro et al. 2018), were not considered if already assigned to other functional systems (i.e. the default mode and fronto-parietal systems, respectively). Thus, it is possible that regions functionally connected with the amygdala—and relevant for prediction—were not assigned to the amygdala system in the current parcellation, resulting in null PSA findings. Alternatively, there may be redundancies in the information encoded by amygdala–visual connections that are encoded in other amygdala–prefrontal connections (e.g. amygdala-cingulo-opercular), as valence-specific neural representations in visual cortex appear to be influenced by anterior (prefrontal) signals (Bo et al. 2021). That said, the nature of the null findings does not provide confirmatory evidence *against* its involvement. Rather, the results are inconclusive.

It is also worth noting the absence of evidence for a role of the salience system. There remains confusion in the literature around distinguishing the salience system (Seeley et al. 2007) from the cingulo-opercular system (Dosenbach et al. 2007). Though both systems are close anatomically, their patterns of RSFC are distinct (see Dosenbach et al. 2007; Power et al. 2011) and there is a clear distinction in the predictive power of the functional systems in the present analyses. Although there is evidence that motivationally salient stimuli—including external emotional signals (e.g. facial expressions)—engage the salience system (Bartels and Zeki 2004; Singer et al. 2004), it appears that the resolution of emotional ambiguity is more related to variation in systems involved in task control, maintenance, and orienting rather than systems relevant for salience detection.

Clinical implications

The findings provide some clinical insight by informing the neural basis of exacerbated negativity (Beck 1976; Williams et al. 2007; Daniel-Watanabe et al. 2022). Because adults with a more negative valence bias are at risk of elevated anxiety (Park et al. 2016) and depression symptoms (Neta and Brock 2021), and adolescents who fail to develop regulatory patterns of frontoamygdalar connectivity also show heightened depression symptoms (Petro et al. 2021), a persistent negative valence bias may represent a transdiagnostic feature. Our results suggest possible neurobiological targets for intervention during the crucial developmental period of adolescence into emerging adulthood (Silvers and Peris 2023).

Certainly, the developmental shift from negativity to greater variation in adulthood could, in theory, arise from numerous neurobiological sources, but our findings point toward specific mechanisms. For example, it could be the case that valence bias is entirely learned from observation of others via intergenerational transmission of learned fear (e.g. seeing parents react negatively to ambiguous situations; Silvers et al. 2021), a learning process that would likely be amygdala-mediated (Schultz et al. 2012; Hermans et al. 2017). Although our findings do not refute such a possibility, and the involvement of the amygdala-cingulo-opercular block provides some evidence of amygdala

involvement, the findings suggest that variation in valence bias is more readily detectable via intrinsic brain organization of task-control and visual systems (in the current parcellation scheme).

The implication of cingulo-opercular and fronto-parietal task-control systems in predicting valence bias suggests that dysregulated control systems underlie the transdiagnostic tendency for individuals with internalizing disorders to remember or attend to negative information (Hamilton and Gotlib 2008; Mitte 2008; Gollan et al. 2016). Relatedly, others report links between cingulo-opercular system connectivity patterns and pediatric anxiety disorders (e.g. generalized anxiety disorder; Becker et al. 2023). As such, future efforts should examine whether cingulo-opercular system activity mediates the association between a more negative valence bias and heightened internalizing symptoms (Park et al. 2016) and whether interventions that shift valence bias (e.g. mindfulness training; Harp et al. 2022; Neta et al. 2023) or disrupt the cingulo-opercular system (e.g. via transcranial magnetic stimulation; Yeager et al. 2021) may reduce persistent negativity.

Strengths, limitations, and future directions

Despite recent suggestions that reproducible associations of between-person brain and behavior relationships require sample sizes greater than 1,000 participants (Marek et al. 2022), we built a cross-validated model in a sample of 119 children and adolescents. As such, we provide evidence that coupling robust and reliable measures that maximize individual differences in behavior, like the valence bias task (Neta et al. 2009, 2013), with rigorous statistical approaches (e.g. cross validation, permutation analyses Nielsen et al. 2019, 2022) can provide sufficient data for predictive models (Spisak et al. 2023).

That said, this work is not without its limitations. Although the use of internal cross-validation maintains the independence of training and testing data in model development, a more rigorous test of the model's generalizability is application to external data (Scheinost et al. 2019). To facilitate this endeavor of future research, we have shared the weights of our model on Open Science Framework (https://osf.io/x8pmc/). In future work, we intend to pursue prediction from task-based fMRI, too, which may explain additional variance in valence bias (Elliott et al. 2019). Further, the role of primary sensory cortices in determining bias could be addressed by delivering auditory presentations of emotionally ambiguous words (Harp et al. 2021).

Conclusion

In brief, we provide a first step toward uncovering the origins of valence bias in childhood and adolescence, a crucial period of development that informs mental health trajectories for decades to come. We show that variation in intrinsic brain organization contributes to individual differences in valence bias, indicating that intrinsic brain organization represents at least one source of variability that explains why some individuals have a more negative bias and others are more positive. Further, the findings provide the first evidence for a role of the cingulo-opercular system in valence bias in childhood and adolescence, an effect that dovetails with research in adults (Neta et al. 2013). Lastly, the results identify a group of functional systems (i.e. cingulo-opercular, fronto-parietal, and visual) that appeared in both the system- and block-level PSAs, and thus may be involved in the regulatory processing that gives rise to individual differences in valence bias. As such, the results provide novel insight into the neural basis of a cognitive–behavioral phenotype of internalizing disorders and directions for future research that will be crucial

in reducing the prevalence and burden of internalizing disorders (Greenberg et al. 2015; Weinberger et al. 2018; American Academy of Child and Adolescent Psychiatry 2021).

Acknowledgments

Supplementary material

Supplementary material is available at *Cerebral Cortex* online.

Author contributions

Nicholas Harp (Formal analysis, Investigation, Visualization, Writing—original draft, Writing—review & editing), Ashley N. Nielsen (Software, Visualization, Writing—review & editing), Douglas Schultz (Resources, Software, Writing—review & editing), and Maital Neta (Conceptualization, Funding acquisition, Investigation, Methodology, Supervision, Writing—review & editing).

Funding

References

Amaral DG, Behniea H, Kelly JL. Topographic organization of projections from the amygdala to the visual cortex in the macaque monkey. *Neuroscience*. 2003:118(4):1099–1120.

American Academy of Child & Adolescent Psychiatry. *Pediatricians, CAPs, and Children's hospitals declare national emergency*. Washington, D.C.: American Academy of Child & Adolescent Psychiatry, 2021. [accessed 2023 May 8]. https://www.aacap.org/aacap/zLatest_News/Pediatricians_CAPs_Childrens_Hospitals_Declare_National_Emergency_Childrens_Mental_Health.aspx.

Andersen SL, Teicher MH. Stress, sensitive periods and maturational events in adolescent depression. *Trends Neurosci*. 2008:31(4):183–191.

Bartels A, Zeki S. The neural correlates of maternal and romantic love. *NeuroImage*. 2004:21(3):1155–1166.

Beck AT. *Cognitive therapy and the emotional disorders*. New York (NY): Meridian; 1976.

Becker HC, Norman LJ, Yang H, Monk CS, Phan KL, Taylor SF, Liu Y, Mannella K, Fitzgerald KD. Disorder-specific cingulo-opercular network hyperconnectivity in pediatric OCD relative to pediatric anxiety. *Psychol Med*. 2023:53(4):1468–1478.

Bo K, Yin S, Liu Y, Hu Z, Meyyappan S, Kim S, Keil A, Ding M. Decoding neural representations of affective scenes in retinotopic visual cortex. *Cereb Cortex*. 2021:31(6):3047–3063.

Bradley MM, Lang PJ. The international affective picture system (IAPS) in the study of emotion and attention. In: Coan JA, Allen JJB, editors. *Handbook of emotion elicitation and assessment*. New York (NY): Oxford University Press; 2007. pp. 29–46.

Brock RL, Harp NR, Neta M. Interpersonal emotion regulation mitigates the link between trait neuroticism and a more negative valence bias. *Personal Individ Differ*. 2022:196:111726.

Brown CC, Raio CM, Neta M. Cortisol responses enhance negative valence perception for ambiguous facial expressions. *Sci Rep*. 2017:7(1):15107.

Bullmore E, Sporns O. Complex brain networks: graph theoretical analysis of structural and functional systems. *Nat Rev Neurosci*. 2009:10(3):186–198.

Cacioppo JT, Hughes ME, Waite LJ, Hawkley LC, Thisted RA. Loneliness as a specific risk factor for depressive symptoms: cross-sectional and longitudinal analyses. *Psychol Aging*. 2006:21(1):140–151.

Casanova R, Whitlow CT, Wagner B, Espeland MA, Maldjian JA. Combining graph and machine learning methods to analyze differences in functional connectivity across sex. *Open Neuroimaging J*. 2012:6:1–9.

Čeko M, Kragel PA, Woo C-W, López-Solà M, Wager TD. Common and stimulus-type-specific brain representations of negative affect. *Nat Neurosci*. 2022:25(6):760–770.

Cox RW, Chen G, Glen DR, Reynolds RC, Taylor PA. FMRI clustering in AFNI: false-positive rates redux. *Brain Connect*. 2017:7(3):152–171.

Craddock RC, Holtzheimer PE, Hu XP, Mayberg HS. Disease state prediction from resting state functional connectivity. *Magn Reson Med Off J Soc Magn Reson Med Soc Magn Reson Med*. 2009:62(6):1619–1628.

Dale AM, Fischl B, Sereno MI. Cortical surface-based analysis I. Segmentation and surface reconstruction. *NeuroImage*. 1999:9(2):179–194.

Daniel-Watanabe L, McLaughlin M, Gormley S, Robinson OJ. Association between a directly translated cognitive measure of negative bias and self-reported psychiatric symptoms. *Biol Psychiatry Cogn Neurosci Neuroimaging*. 2022:7(2):201–209.

Dosenbach NUF, Fair DA, Cohen AL, Schlaggar BL, Petersen SE. A dual-networks architecture of top-down control. *Trends Cogn Sci*. 2008:12(3):99–105.

Dosenbach NUF, Fair DA, Miezin FM, Cohen AL, Wenger KK, Dosenbach RAT, Fox MD, Snyder AZ, Vincent JL, Raichle ME, et al. Distinct brain networks for adaptive and stable task control in humans. *Proc Natl Acad Sci*. 2007:104(26):11073–11078.

Dunkley DM, Lewkowski M, Lee IA, Preacher KJ, Zuroff DC, Berg J-L, Foley JE, Myhr G, Westreich R. Daily stress, coping, and negative and positive affect in depression: complex trigger and maintenance patterns. *Behav Ther*. 2017:48(3):349–365.

Dworetsky A, Seitzman BA, Adeyemo B, Neta M, Coalson RS, Petersen SE, Gratton C. Probabilistic mapping of human functional brain networks identifies regions of high group consensus. *NeuroImage*. 2021:237:118164.

Elliott ML, Knodt AR, Cooke M, Kim MJ, Melzer TR, Keenan R, Ireland D, Ramrakha S, Poulton R, Caspi A, et al. General functional connectivity: shared features of resting-state and task fMRI drive reliable and heritable individual differences in functional brain networks. *NeuroImage*. 2019:189:516–532.

Eysenck MW, Mogg K, May J, Richards A, Mathews A. Bias in interpretation of ambiguous sentences related to threat in anxiety. *J Abnorm Psychol*. 1991:100(2):144–150.

Finn ES, Shen X, Scheinost D, Rosenberg MD, Huang J, Chun MM, Papademetris X, Constable RT. Functional connectome fingerprinting: identifying individuals using patterns of brain connectivity. *Nat Neurosci*. 2015:18(11):1664–1671.

Fox MD, Raichle ME. Spontaneous fluctuations in brain activity observed with functional magnetic resonance imaging. *Nat Rev Neurosci*. 2007:8(9):700–711.

Freeman JB, Ambady N. MouseTracker: software for studying real-time mental processing using a computer mouse-tracking method. *Behav Res Methods*. 2010:42(1):226–241.

Friston KJ, Williams S, Howard R, Frackowiak RS, Turner R. Movement-related effects in fMRI time-series. *Magn Reson Med*. 1996:35(3):346–355.

Gee DG, Humphreys KL, Flannery J, Goff B, Telzer EH, Shapiro M, Hare TA, Bookheimer SY, Tottenham N. A developmental shift from positive to negative connectivity in human amygdala-prefrontal circuitry. *J Neurosci*. 2013:33(10):4584–4593.

Gollan JK, Hoxha D, Hunnicutt-Ferguson K, Norris CJ, Rosebrock L, Sankin L, Cacioppo J. The negativity bias predicts response rate to behavioral activation for depression. *J Behav Ther Exp Psychiatry*. 2016:52:171–178.

Gordon EM, Laumann TO, Adeyemo B, Huckins JF, Kelley WM, Petersen SE. Generation and evaluation of a cortical area parcellation from resting-state correlations. *Cereb Cortex*. 2016:26(1):288–303.

Gratton C, Neta M, Sun H, Ploran EJ, Schlaggar BL, Wheeler ME, Petersen SE, Nelson SM. Distinct stages of moment-to-moment processing in the Cinguloopercular and Frontoparietal networks. *Cereb Cortex*. 2017:27(3):2403–2417.

Greenberg PE, Fournier A-A, Sisitsky T, Pike CT, Kessler RC. The economic burden of adults with major depressive disorder in the United States (2005 and 2010). *J Clin Psychiatry*. 2015:76(2):155–162.

Hamilton JP, Gotlib IH. Neural substrates of increased memory sensitivity for negative stimuli in major depression. *Biol Psychiatry*. 2008:63(12):1155–1162.

Harp NR, Brown CC, Neta M. Spring break or heart break? Extending valence bias to emotional words. *Soc Psychol Personal Sci*. 2021:12(7):1392–1401.

Harp NR, Freeman JB, Neta M. Mindfulness-based stress reduction triggers a long-term shift toward more positive appraisals of emotional ambiguity. *J Exp Psychol Gen*. 2022:151(9):2160–2172.

Harp NR, Gross JJ, Uusberg A, Neta M. The role of trait reappraisal in response to emotional ambiguity: a meta-analysis. *Emotion*. 2023: Advance online publication.

Harp NR, Neta M. Tendency to share positive emotions buffers loneliness-related negativity in the context of shared adversity. *J Res Personal*. 2023:102:104333.

Hermans EJ, Kanen JW, Tambini A, Fernández G, Davachi L, Phelps EA. Persistence of amygdala-hippocampal connectivity and multi-voxel correlation structures during awake rest after fear learning predicts long-term expression of fear. *Cereb Cortex*. 2017:27(5):3028–3041.

Kim H, Somerville LH, Johnstone T, Alexander AL, Whalen PJ. Inverse amygdala and medial prefrontal cortex responses to surprised faces. *Neuroreport*. 2003:14(18):2317–2322.

Kragel PA, Reddan MC, LaBar KS, Wager TD. Emotion schemas are embedded in the human visual system. *Sci Adv*. 2019:5(7):eaaw4358.

Krieglmeyer R, Deutsch R, De Houwer J, De Raedt R. Being moved: valence activates approach-avoidance behavior independently of evaluation and approach-avoidance intentions. *Psychol Sci*. 2010:21(4):607–613.

Laumann TO, Snyder AZ. Brain activity is not only for thinking. *Curr Opin Behav Sci*. 2021:40:130–136.

Lundqvist D, Flykt A, Öhman A. *The Karolinska directed emotional faces - KDEF, CD ROM*. [accessed 2022 Sep 21]. Stockholm: Karolinska Institute, Department of Clinical Neuroscience, Psychology Section, 1998. https://www.kdef.se/home/aboutKDEF.html.

Marek S, Tervo-Clemmens B, Calabro FJ, Montez DF, Kay BP, Hatoum AS, Donohue MR, Foran W, Miller RL, Hendrickson TJ, et al. Reproducible brain-wide association studies require thousands of individuals. *Nature*. 2022:603(7902):654–660.

Marusak HA, Zundel CG, Brown S, Rabinak CA, Thomason ME. Convergent behavioral and corticolimbic connectivity evidence of a negativity bias in children and adolescents. *Soc Cogn Affect Neurosci*. 2017:12(4):517–525.

Mitte K. Memory bias for threatening information in anxiety and anxiety disorders: a meta-analytic review. *Psychol Bull*. 2008:134(6):886–911.

Neta M, Berkebile MM, Freeman JB. The dynamic process of ambiguous emotion perception. *Cogn Emot*. 2021:35(4):722–729.

Neta M, Brock RL. Social connectedness and negative affect uniquely explain individual differences in response to emotional ambiguity. *Sci Rep*. 2021:11(1):3870.

Neta M, Dodd MD. Through the eyes of the beholder: simulated eye-movement experience ("SEE") modulates valence bias in response to emotional ambiguity. *Emotion*. 2018:18(8):1122–1127.

Neta M, Harp NR, Henley DJ, Beckford SE, Koehler K. One step at a time: physical activity is linked to positive interpretations of ambiguity. *PLoS One*. 2019:14(11):e0225106.

Neta M, Harp NR, Tong TT, Clinchard CJ, Brown CC, Gross JJ, Uusberg A. Think again: the role of reappraisal in reducing negative valence bias. *Cogn Emot*. 2023:37(2):238–253.

Neta M, Kelley WM, Whalen PJ. Neural responses to ambiguity involve domain-general and domain-specific emotion processing systems. *J Cogn Neurosci*. 2013:25(4):547–557.

Neta M, Nelson SM, Petersen SE. Dorsal anterior cingulate, medial superior frontal cortex, and anterior insula show performance reporting-related late task control signals. *Cereb Cortex*. 2016:27(3):bhw053–bh2165.

Neta M, Norris CJ, Whalen PJ. Corrugator muscle responses are associated with individual differences in positivity-negativity bias. *Emotion*. 2009:9(5):640–648.

Neta M, Schlaggar BL, Petersen SE. Separable responses to error, ambiguity, and reaction time in cingulo-opercular task control regions. *NeuroImage*. 2014:99:59–68.

Neta M, Tong TT, Rosen ML, Enersen A, Kim MJ, Dodd MD. All in the first glance: first fixation predicts individual differences in valence bias. *Cogn Emot*. 2017:31(4):772–780.

Neta M, Whalen PJ. The primacy of negative interpretations when resolving the valence of ambiguous facial expressions. *Psychol Sci*. 2010:21(7):901–907.

Nielsen AN, Barch DM, Petersen SE, Schlaggar BL, Greene DJ. Machine learning with neuroimaging: evaluating its applications in psychiatry. *Biol Psychiatry Cogn Neurosci Neuroimaging*. 2020:5(8): 791–798.

Nielsen AN, Greene DJ, Gratton C, Dosenbach NUF, Petersen SE, Schlaggar BL. Evaluating the prediction of brain maturity from functional connectivity after motion Artifact Denoising. *Cereb Cortex*. 2019:29(6):2455–2469.

Nielsen AN, Kaplan S, Meyer D, Alexopoulos D, Kenley JK, Smyser TA, Wakschlag LS, Norton ES, Raghuraman N, Warner BB, et al. Maturation of large-scale brain systems over the first month of life. *Cereb Cortex*. 2022:33(6):2788–2803.

Norris CJ, Larsen JT, Crawford LE, Cacioppo JT. Better (or worse) for some than others: individual differences in the positivity offset and negativity bias. *J Res Personal*. 2011:45(1):100–111.

Park G, Vasey MW, Kim G, Hu DD, Thayer JF. Trait anxiety is associated with negative interpretations when resolving valence ambiguity of surprised faces. *Front Psychol*. 2016:7:1164.

Petro NM, Tong TT, Henley DJ, Neta M. Individual differences in valence bias: fMRI evidence of the initial negativity hypothesis. *Soc Cogn Affect Neurosci*. 2018:13(7):687–698.

Petro NM, Tottenham N, Neta M. Exploring valence bias as a metric for frontoamygdalar connectivity and depressive symptoms in childhood. *Dev Psychobiol*. 2021:63(5):1013–1028.

Phillips ML, Ladouceur CD, Drevets WC. A neural model of voluntary and automatic emotion regulation: implications for understanding the pathophysiology and neurodevelopment of bipolar disorder. *Mol Psychiatry*. 2008:13(9):829, 833–829, 857.

Power JD, Cohen AL, Nelson SM, Wig GS, Barnes KA, Church JA, Vogel AC, Laumann TO, Miezin FM, Schlaggar BL, et al. Functional network organization of the human brain. *Neuron*. 2011:72(4):665–678.

Power JD, Mitra A, Laumann TO, Snyder AZ, Schlaggar BL, Petersen SE. Methods to detect, characterize, and remove motion artifact in resting state fMRI. *NeuroImage*. 2014:84:320–341.

Puccetti NA, Villano WJ, Stamatis CA, Hall KA, Torrez VF, Neta M, Timpano KR, Heller AS. Negative interpretation bias connects to real-world daily affect: a multistudy approach. *J Exp Psychol Gen*. 2023:152(6):1690–1704.

Raio CM, Harp NR, Brown CC, Neta M. Reappraisal-but not suppression-tendencies determine negativity bias after laboratory and real-world stress exposure. *Affect Sci*. 2021:2(4):455–467.

Santarnecchi E, Galli G, Polizzotto NR, Rossi A, Rossi S. Efficiency of weak brain connections support general cognitive functioning. *Hum Brain Mapp*. 2014:35(9):4566–4582.

Scheinost D, Noble S, Horien C, Greene AS, Lake EM, Salehi M, Gao S, Shen X, O'Connor D, Barron DS, et al. Ten simple rules for predictive modeling of individual differences in neuroimaging. *NeuroImage*. 2019:193:35–45.

Schultz D, Balderston N, Helmstetter F. Resting-state connectivity of the amygdala is altered following Pavlovian fear conditioning. *Front Hum Neurosci*. 2012:6:242.

Seeley WW, Menon V, Schatzberg AF, Keller J, Glover GH, Kenna H, Reiss AL, Greicius MD. Dissociable intrinsic connectivity networks for salience processing and executive control. *J Neurosci*. 2007:27(9):2349–2356.

Silvers JA, Callaghan BL, VanTieghem M, Choy T, O'Sullivan K, Tottenham N. An exploration of amygdala-prefrontal mechanisms in the intergenerational transmission of learned fear. *Dev Sci*. 2021:24(3):e13056.

Silvers JA, Peris TS. Research review: the neuroscience of emerging adulthood – reward, ambiguity, and social support as building blocks of mental health. *J Child Psychol Psychiatry*. 2023:64(7):989–997.

Singer T, Seymour B, O'Doherty J, Kaube H, Dolan RJ, Frith CD. Empathy for pain involves the affective but not sensory components of pain. *Science*. 2004:303(5661):1157–1162.

Spisak T, Bingel U, Wager TD. Multivariate BWAS can be replicable with moderate sample sizes. *Nature*. 2023:615(7951):E4–E7.

Sterzer P, Russ MO, Preibisch C, Kleinschmidt A. Neural correlates of spontaneous direction reversals in ambiguous apparent visual motion. *NeuroImage*. 2002:15(4):908–916.

Ströhle A. Physical activity, exercise, depression and anxiety disorders. *J Neural Transm (Vienna)*. 2009:116(6):777–784.

Talairach J, Tournoux P. Co-planar stereotaxic atlas of the human brain: 3-Dimensional proportional system: An approach to cerebral imaging. New York: Thieme Medical Publishers, *Inc*, 1988.

Van Essen DC, Glasser MF, Dierker DL, Harwell J, Coalson T. Parcellations and hemispheric asymmetries of human cerebral cortex analyzed on surface-based atlases. *Cereb Cortex*. 2012:22(10):2241–2262.

Yeo BT, Krienen FM, Sepulcre J, Sabuncu MR, Lashkari D, Hollinshead M, Roffman JL, Smoller JW, Zöllei L, Polimeni JR, et al. The organization of the human cerebral cortex estimated by intrinsic functional connectivity. *J Neurophysiol*. 2011:106(3):1125–1165.

Thompson-Schill SL, D'Esposito M, Aguirre GK, Farah MJ. Role of left inferior prefrontal cortex in retrieval of semantic knowledge: a reevaluation. *Proc Natl Acad Sci USA*. 1997:94(26):14792–14797.

Tottenham N, Phuong J, Flannery J, Gabard-Durnam L, Goff B. A negativity bias for ambiguous facial expression valence during childhood: converging evidence from behavior and facial corrugator muscle responses. *Emot Wash DC*. 2013:13(1):92–103.

Tottenham N, Tanaka JW, Leon AC, McCarry T, Nurse M, Hare TA, Marcus DJ, Westerlund A, Casey BJ, Nelson C. The NimStim set of facial expressions: judgments from untrained research participants. *Psychiatry Res*. 2009:168(3):242–249.

Tversky A, Kahneman D. Belief in the law of small numbers. *Psychol Bull*. 1971:76(2):105–110.

Weinberger AH, Gbedemah M, Martinez AM, Nash D, Galea S, Goodwin RD. Trends in depression prevalence in the USA from 2005 to 2015: widening disparities in vulnerable groups. *Psychol Med*. 2018:48(8):1308–1315.

Williams LM, Kemp AH, Felmingham K, Liddell BJ, Palmer DM, Bryant RA. Neural biases to covert and overt signals of fear: dissociation by trait anxiety and depression. *J Cogn Neurosci*. 2007:19(10):1595–1608.

Yeager BE, Dougher CC, Cook RH, Medaglia JD. The role of transcranial magnetic stimulation in understanding attention-related networks in single subjects. *Curr Res Neurobiol*. 2021:2:100017.